Packing potential index for binary mixtures of granular soil

Packing potential index for binary mixtures of granular soil

Ching S. Chang[1], Yibing Deng[2]

[1]Professor, Department of Civil and Environmental Engineering, University of Massachusetts, Amherst, MA 01003 (corresponding author). E-mail: cchang@engin.umass.edu;

[2]Graduate student, Department of Civil and Environmental Engineering, University of Massachusetts, Amherst, MA 01003. E-mail: yibingdeng@engin.umass.edu;

ABSTRACT

Packing procedure is the mechanical process of forming a packing of soil particles, such as funnel pouring, tamping, rodding, pluviation, compaction, vibration, compression, etc. For a sand-silt mixture, packing procedure and particle shape have significant effects on the density of the binary mixture. However, these two factors have not been considered in most of the existing particle packing density models. Thus, the existing particle packing density models are not applicable to sand-silt mixtures. In this paper, we aim to study the packing procedure and particle shape effects on density of binary mixtures. We firstly define a packing potential index, which is a measure of volume reduction potential due to mixing of two components of a binary mixture system under a packing procedure. To understand the nature of packing potential index, we compare the packing potential indices of 24 different types of mixtures collected from the literature; the 24 types of mixtures were formed by two different types of packing procedure (i.e., for achieving minimum and maximum void ratios). It is found that the packing potential index is nearly independent of packing procedure but significantly dependent on the compound particle shapes of a mixture. Then, we mathematically link the packing potential index to the particle interaction parameters used in the particle packing density models. And we analyze the data to discuss the effect of packing procedure on the void ratios of sand-silt mixtures. We then

propose an approach within the framework of particle packing density model to predict the void ratios of sand-silt mixtures under different packing procedures with the consideration of particle shape effect.

Key words: Particle packing model; minimum and maximum void ratios; sand-silt mixture; particle shape; packing procedure

1. Introduction

The paper is motivated by problems of silty sand from soil mechanics, in which, the variable of void ratio, instead of packing density, is commonly used. The void ratio e can be related to the packing density ϕ by: $\phi = 1/(1+e)$ or $e = (1/\phi) - 1$.

There are several analytical models to study the void ratios of binary particle mixtures in many branches of industry, such as ceramics processing [1], powder metallurgy [2], and concrete mixes [3]. Among these models, the most popular ones are based on the hypothesis of two mechanisms of particle arrangements [4,5]: (i) the filling mechanism of the fine particles filling into voids among coarse particles; (ii) the embedment mechanism of coarse particles occupying solid volumes in place of porous bulk volumes of the fine particles. The filling mechanism occurs for mixtures with low fines contents; and the embedment mechanism occurs for mixtures with high fines contents. In these two mechanisms, the models did not consider particle interactions that cause packing disturbance; thus, the models only provide good estimates of lower bound solutions.

These models were then evolved to consider the effect of particle interaction. During filling of fine particles, loosening of the coarse particle network may occur when fine particles are pushed into the voids

among coarse particles. On the other hand, during embedment of coarse particles, disrupting the packing of fine particles may occur at the wall-like boundaries of coarse particles. The packing model introduced by Powers [3] considers the loosening effect. The packing models developed by Aïm and Goff [6] and Toufar et al. [7] account for the wall effect. The packing models developed by Yu et al. [8], Goltermann et al. [9], Stovall et al. [10], De Larrard [11], Dewar [12], and Kwan et. al [13] take into account of both the loosening and wall effects.

The loosening and wall effects have been found to be significantly affected by particle size ratio *r* (i.e., ratio of fine to coarse particle sizes) [14]. Thus, the effects are expressed as particle interaction functions dependent on the particle size ratio. The two parameters (*a* and *b*) in the particle interaction functions were obtained by regression analysis of experimental results on packing densities for mixtures with different size ratios. The interaction parameters and interaction functions derived in the models by Yu et al. [8], De Larrard [11], and Kwan [13] have different forms.

It is obvious that the loosening and wall effects can be affected by other factors of particle morphology, such as particle shape, roundness and surface texture roughness. Among several aspects of morphology, the particle shape has been considered in the model by Yu et al. [8], however, the particle shape considered was simple idealized nonspherical shape (e.g., cylinders, disks). For most material, the particle morphology is complex and difficult to be measured quantitatively. Hence, from either a theoretical or a practical point of view, the complex particle morphology cannot be considered in the model in a fully satisfied manner. And most currently available models do not consider factors of particle morphology. Because of this limitation in models, the evaluation of several models by Jones [15] indicated that each of these models is applicable only to a certain type of industrial material. Also indicated by Chang et al. [16], due to a large span of size and shape differences, the parameters used in these models are not suitable for sand-silt mixtures.

69 Furthermore, the complexity involves not only particle morphology, but also the packing procedure (i.e.,
70 method of mixing, placement and compaction), by which the binary packing is physically formed. The factor
71 of packing procedure is not addressed in most binary packing models. De Larrard [11] developed the
72 ‘‘compressible packing model” (CPM) by introducing the compaction index K, which is assumed to be
73 related to the applied compaction effort, thus is dependent on the packing procedure. The value of K is an
74 empirical parameter varying from 4 to 9 suggested for pouring, rodding, vibration and compression, and is
75 also varying with grain shape (round & crushed) [11]. He proposed a method to convert the virtual packing
76 density to the actual packing density through the compaction index. But the CPM is not suitable for
77 geotechnical material such as silty sand [16].

78 In geotechnical engineering, minimum and maximum void ratios (e_{max} and e_{min}), which represent the
79 densest and loosest states of a soil mixture, are widely applied in earthwork design and planning. The
80 packing procedures of achieving e_{max} and e_{min} are very different. Thus, to understand the effect of the
81 packing procedures on the density of mixtures is important in geotechnical engineering.

82 In this paper, we aim to study the effects of particle shape and packing procedure on densities of binary
83 mixtures. We firstly define a packing potential index, the value of which is a number between 0 and 1. This
84 index is a measure of void reduction potential due to mixing of two components of a binary mixture under a
85 packing procedure. To study how the packing potential index may vary with the type of mixtures and with
86 the type of packing procedure, we compare the packing potential indices for 24 systems of soil mixtures
87 collected from the literature; the 24 systems of mixtures were formed under two different types of packing
88 procedure (i.e., for achieving minimum and maximum void ratios).

89 Then, we mathematically derive the relationship between the packing potential index and the particle
90 interaction parameters, and analyze the data to discuss the effect of packing procedure on void ratio of

91 mixtures. Finally, we discuss an approach, under the framework of particle packing model, for predicting
92 void ratio (e_{max} and e_{min}) of a mixture under different packing procedures with the consideration of particle
93 shape effect.
94
95 **2. Packing potential index**
96 Consider a binary packing mixture composed of 2 groups of particles. The particle sizes for the two
97 groups are denoted by d_1 and d_2, respectively (note that $d_1 \geqslant d_2$). The solid volume fractions of the two
98 groups of particles are denoted by y_1 and y_2, respectively (note that $y_1 + y_2 = 1$).
99 We aim to determine the void ratio *e* of a binary soil mixture based on the monodisperse void ratios of the
100 two components (e_1 and e_2). Note that the void ratios, *e*, e_1 and e_2, are measured from three packings formed
101 by the same packing procedure.
102 The void ratio *e* of a binary soil mixture is between the upper bound and lower bound void ratios, which
103 can be constructed by the monodisperse void ratios of the two components (e_1 and e_2). The upper bound
104 void ratio, e^U, is hypothesized to be the Voigt average of the monodisperse void ratios, given by

105 $$e^U = e_1 y_1 + e_2 y_2 \quad (1)$$

106 The upper bound is plotted as line AB in Fig. 1, in which the fines content, $f_c = y_2$.
107 In contrast, the lower bound void ratio, e^L, is derived by assuming that the two groups of particles in the
108 mixture have no interactions [4,5]. There are two scenarios: (1) every fine particle exists only in the void
109 space between coarse particles (i.e., in the coarse particle dominant region), which is shown as line AC in
110 Fig. 1, or (2) every coarse particle is fully dispersed in the matrix of fine particles (i.e., in the fine particle
111 dominant region), which is shown as line CB in Fig. 1. The equations for AC and CB are given respectively
112 by

113 $$e^L = e_1 - (1 + e_1)y_2 \; ; \qquad e^L = e_2 y_2 \qquad (2)$$

114 The slope of AC is -(1+ e_1) and the slope of CB is e_2 as shown in Fig. 1. The line ACB is the lower
115 bound.

116 < Fig.1 >

117 For a system of mixtures (i.e., mixtures with the same two components of various combinations), the void
118 ratios of the binary mixtures with various f_c are between the upper and the lower bounds as the curve ADB
119 shown in Fig. 1. For convenient, we define a packing potential index Ω as the ratio of area ADB to area
120 ACB, which is a material descriptor for a system of mixtures. This index is a measure of volume reduction
121 potential due to mixing of two components of a binary mixture system under a packing procedure, which is a
122 simple scaler and can be directly obtained from experimental data. Thus, it is convenient to be used for
123 studying the effect of particle shape and packing procedure. The value of packing potential index Ω is
124 between 0 and 1. The higher value of Ω indicates a higher potential of volume reduction of the mixtures.

125 For the case of $e_1 = e_2$, the monodisperse void ratio is same for both components and is the upper bound.
126 Under the same packing procedure, the binary mixtures, for all fines content, can generally be packed to a
127 denser packing than the monodisperse packing. The packing potential index Ω indicates roughly how much
128 denser the binary mixtures can be effectively achieved compared to the monodisperse packing.

129 The purpose of a packing density model is to predict the void ratio *e* of a binary mixture based on the
130 values e_1 and e_2 of the monodisperse packings. Thus, it is important to study various factors that affect the
131 packing potential index.

132

3. Factors affect packing potential index

3.1. *Effect of particle morphology*

The packing potential index is significantly affected by particle size ratio r (i.e., $r = d_2/d_1$, the particle size of fine particles divided by the particle size of coarse particles) as indicated in the test results of spherical steel shots by McGeary [14] and in the test results of spherical glass beads by Kwan et al. [13], as shown in Fig. 2a and Fig 2b. Steel shots and glass beads are round particles. The particle size range is from 0.16mm to 3.14mm for steel shots, and from 1.43mm to 15.73mm for glass beads. The packing potential index is plotted for mixtures with various size ratio in Fig. 2c. The size ratio of fine particles to coarse particles ranges from 0.05 to 0.75. For binary mixtures with small size ratios ($d_1 >> d_2$), the packing potential indices are nearly 1, meaning that the mixture is more capable of specific volume reduction and can be packed approaching the lower bound solution. Whereas, for mixtures with large size ratios ($d_1 \approx d_2$), the packing potential indices are nearly zero, and the void ratios of the mixtures can be achieved approaching to the upper bound.

< Fig.2 >

It is noted that, for a binary mixture of steel shots or of glass beads, the mixture is composed of two groups of mono-sized particles. However, for silty-sand, the two groups of particles are not mono-sized. The sand particles are relatively uniform, but the silt particles usually have a wider range of sizes. Thus, the sand-silt mixture is a deviation from the standard meaning of binary mixtures defined in particle packing models. However, in this study, we have neglected this factor because the grain size distribution of silt is seldom measured in geotechnical practice, and the information on measured void ratios of mono sized silt is not available in the literature. The mean particle size for sand or silt is referred to as the particle size denoted by d_1 or d_2 in this study.

155 Besides particle size ratio, it is reasonable to expect that particle morphology is also a crucial factor that
156 influences the packing potential index. There are many aspects of particle morphology, which can be
157 generally expressed in terms of elongation ratio (i.e., aspect ratio), roundness, sphericity, angularity and
158 surface roughness [17]. At a larger scale, the term ‘‘sphericity” is used to characterize the overall shape of the
159 granular particle by a measure of the degree of conformity of particle shape to that of sphere circumscribing
160 the particle [19]. At a smaller scale, the term “roundness” defined by Wadell [20] is used to describe the
161 degree of sharpness of particle edges/corners. At an even smaller scale, surface roughness [21] is used to
162 describe the surface texture. There is no consensus on which descriptor is better to characterize the particle
163 morphology, for example of the overall particle shape alone, there are three measures: aspect ratio,
164 sphericity, angularity, etc.

165 Although digital image analysis and computed tomography techniques have been employed to
166 quantitatively characterize the aggregate morphology [22], in general practice, the morphology parameters are
167 often not measured in experiments. In most test results presented in the literature, only qualitative descriptors
168 of particle shapes (such as round, angular, sub-angular, etc.) are provided.

169 Fig. 3 illustrates the measured void ratios and the calculated upper and lower bounds for 3 systems of
170 mixtures under the same packing condition. The compound particle shapes are denoted as coarse particle
171 shape/ fine particle shape for the following 3 systems of mixtures: Steel shots (round/round), Silica sand-silt
172 (subangular/subangular), and Cambria-Nevada sand-silt (round/angular). Note that the particle size ratios for
173 these 3 systems of mixtures are nearly same, but the three packing potential indices are different as shown in
174 Fig. 3. The shapes of coarse particles and fine particles are similar for steel shots and silica sand-silt, whereas
175 different for Cambria-Nevada sand-silt. Because of the effect of particle shape the three packing potential
176 indices do not follow the curves of sphere particles previously shown in Fig. 2c. Hence, not only the particle

177 shape of a single component but also the compound particle shapes of two components have significant
178 effect on the packing potential index.

179 < Fig.3 >

180 To further investigate the effect of particle shape, 13 sets of spherical particles binary mixtures and 24 sets
181 of sand-silt mixtures from the literature are collected (see Table 1) for studying the packing potential index as
182 a function of particle shape in a qualitative way. The compound particle shapes of the 37 systems of mixtures
183 are classified into three groups: round/round (R/R), angular/angular or subangular/subangular (A/A, SA/SA),
184 and round/ angular or round/subangular (R/A, R/SA). The computed packing potential indices versus particle
185 size ratio are shown in Fig. 4 for the three groups of compound particle shapes. Fig. 4 shows that the effect
186 of particle shape is significant on the values of packing potential index. As shown in Fig. 4, given a particle
187 size ratio, for binary mixtures composed of two similar shape components, the packing potential index Ω of a
188 R/R mixture is greater than that of a A/A or SA/SA mixture. The packing potential index Ω of a mixture
189 composed of two different shape components is usual smaller than that of a mixture composed of two similar
190 shape components.

191 < Fig.4 >

192 < Table1 >

193

194 3.2. *Effect of packing procedure*

195 In geotechnical engineering, the loosest and densest density states (i.e., maximum and minimum void
196 ratios) of soil are of interest. Several packing procedures have been used for the two limiting void ratios,
197 such as moist tamping, vibratory table, customized sample preparation method, or a combination of these
198 methods. Among these processes, two standards process specifications (ASTM) [30,31] are most commonly

199 used, in which the loosest state (maximum void ratio) is achieved by a process of funnel pouring, in which a
200 funnel is used to pour the dry material into a mould, and slowly turn the mould upside down. Whereas, the
201 densest state is achieved by vibration method with a static weight. It is noted that, before either packing
202 procedure is applied, the particles are thoroughly mixed for all the fractions [32].

203 The three systems of mixtures (in Fig. 5) are used to examine the effect of packing procedure. Fig. 5a
204 shows the void ratios of mixtures achieved by "minimum void ratio" packing procedure, and Fig. 5b shows
205 the void ratios of mixtures achieved by "maximum void ratio" packing procedures. The two different
206 packing procedures have significant effect not only on the void ratios of monodisperse packings but also on
207 the void ratios of binary mixture packings.

208 The packing potential indices are different for different systems of mixtures as shown in Fig. 5: the
209 packing potential index is high for the silica sand-silt mixture, medium for the Ottawa sand-Nevada silt
210 mixture, and low for the Vietnam mixture. However, it is interesting to observe that for each system of
211 mixtures, the packing potential index is nearly same between the two different procedures. Thus, the
212 dependence of the packing potential index on the packing procedure may be very weak.

213 < Fig.5 >

214 To further examine the influence of packing procedure on the packing potential index, the 24 systems of
215 mixtures listed in Table 1 were analyzed. The packing potential indices obtained from the "minimum void
216 ratio" packing procedure ($\Omega_{\min}$) are plotted in Fig. 6 versus the packing potential index obtained from the
217 "maximum void ratio" packing procedure ($\Omega_{\max}$). The correlation between the two packing potential indices
218 is very strong with a coefficient of determination R^2= 0.91. Thus, based on the results of the 24 systems of
219 mixtures, packing potential index has a very weak dependence on packing procedure. Consequently, the
220 packing potential index can be treated as a material property, dependent only on the system of mixtures.

221 It is interesting to note that packing procedure has a significant influence on the packing density, but
222 very small influence on the packing potential index. That means, for a system of mixtures, the upper and
223 lower bound densities are affected by the packing procedure, but the mixture densities relative to the upper
224 and lower bounds are not affected by the packing procedure. This characteristic is helpful for modeling
225 mixture densities due to different packing procedures.
226 < Fig.6 >
227
228 **4. Role of packing potential in particle packing model**
229 Most particle packing density models available in the literature [8, 10, 13, 28] have the similar approach,
230 which is a two-step process: (1) develop upper bound and lower bound void ratios based on the given
231 monodisperse void ratios e_1 and e_2, for packings of coarse and fine particles, and (2) determine the void
232 ratio e of the mixture based on the upper and lower bounds, using the particle interaction parameters. Note
233 that the packing potential is a measure that represents the position of the void ratio e relative to the upper
234 bound and lower bound. Thus, the packing potential parameters and particle interaction parameters have the
235 same physical meaning and the same purpose. In the following, we aim to find the relationship between the
236 packing potential parameters and the particle interaction parameters.
237 4.1. *Linear particle packing model*
238 As defined previously in Fig. 1, the packing potential index Ω is a material property for a system of
239 mixtures (i.e., mixtures with the same two components of various combinations). In order to reveal the effect
240 of fines content of each mixture, we define a packing potential parameter ω for a mixture with specific fines
241 content f_c. Fig. 7a shows a data point D, which represents a mixture with fines content f_c, the packing
242 potential parameter ω is defined by

$$\omega = (e^U - e)/(e^U - e^L) \quad (3)$$

The value of ω represents the position of the void ratio e relative to the upper bound and lower bound void ratios (i.e. e^U and e^L). The parameter ω is dependent on e^U and e^L, which are functions of fines content, given in Eqs. (1) and (2). The area ratio Ω as shown in Fig. 1 can be treated as the average of ω over the all range of fines content f_c.

$$\Omega = \int_0^1 \omega(f_c)\, df_c \quad (4)$$

< Fig.7 >

The void ratio e for the mixture in Eq. (3) can be expressed as

$$e = e^U - \omega(e^U - e^L) \quad (5a)$$

It is noted that, in Fig. 7a, the upper bound is a straight line, but the lower bound has two segments separated by the transitional fines content f_{c1} and the measured test results has two segments separated by the transitional fines content f_{c2}. The coarse particle dominant region can be defined by $f_c < f_{c1}$ and the fine particle dominant region can be defined by $f_c > f_{c2}$. The region in $f_{c1} < f_c < f_{c2}$ is considered as transition zone. Thus, from Eq. (1) and Eq. (2), the value of $(e^U - e^L)$ is different for the two dominant regions:

$$e^U - e^L = (1 + e_2)y_2 \quad \text{for } f_c < f_{c1} \quad (5b)$$

$$e^U - e^L = e_1 y_1 \quad \text{for } f_c > f_{c2} \quad (5c)$$

The value of ω for a mixture in the coarse particle dominant region ($f_c < f_{c1}$) is different from for a mixture in the fine particle dominant region ($f_c > f_{c2}$). They are termed as ω_a and ω_b, respectively. Thus Eq. (5a) becomes

$$e = (e_1 y_1 + e_2 y_2) - \omega_a (1 + e_2) y_2 \quad \text{for } f_c < f_{c1} \quad (6a)$$

$$e = (e_1 y_1 + e_2 y_2) - \omega_b e_1 y_1 \qquad \text{for } f_c > f_{c2} \qquad (6b)$$

If ω_a and ω_b are two constants, Eqs. (6a) and (6b) represent two linear lines. Therefore, if we approximate the data by a bilinear line as shown in Fig. 7a, then in the range of $f_c < f_{c1}$, ω_a is a constant, and in the range of $f_c > f_{c2}$, ω_b is another constant as shown in Fig. 7b. In the range of $f_{c2} > f > f_{c1}$, ω is a transition value from ω_a to ω_b.

The ω calculated directly from experimental data reported by Lade et al. [24] is shown as the symbol of circles in Fig. 7b. The ω calculated from the bilinear line, is shown as the solid curve in Fig. 7b. In the coarse particle dominant region, ω_a is a constant of 0.39. In the fine particle dominant region, ω_b is a different constant of 0.65. In the transition zone, ω varies from 0.39 to 0.65.

It is noted that Eq. (6a) and Eq. (6b) have the similar form as the linear particle packing density models (LPDM) [8–12,16]. These models consider interaction parameters (i.e. the loosening parameter *a* and wall parameter *b*), which always predicts a bilinear packing void ratio curve for a binary mixture as shown in Fig. 7a. Compared with these linear packing models, the packing potential parameter ω_a corresponds to the loosening parameter, and parameter ω_b corresponds to the wall parameter. Precisely, the packing potential parameters can be related to the particle interaction parameters by: $\omega_a = 1 - a$, and $\omega_b = 1 - b$.

These two parameters, as shown in the test results on glass beads and steel shots (see Fig. 2a), are significantly dependent on the particle size ratio *r* (i.e., ratio of fine to coarse particle sizes), which can be obtained by regression analysis of the packing density experimental results for different mixtures.

The interaction functions derived by Yu et al. [8] for their two interaction parameters:

$$a = 1 - (1 - r)^{3.3} - 2.8r(1 - r)^{2.7} \qquad (7a)$$

$$b = 1 - (1 - r)^{2} - 0.4r(1 - r)^{3.7} \qquad (7b)$$

The interaction functions derived by De Larrard [11] for the interaction parameters in CPM:

$$a = \sqrt{1-(1-r)^{1.02}} \tag{8a}$$

$$b = 1-(1-r)^{1.5} \tag{8b}$$

4.2. *Nonlinear particle packing model*

Models that considering the loosening parameter a and wall parameter b can be collectively classified as a 2-parameter model, which includes most of the linear particle packing density models (LPDM) [8–12,16]. As shown in Fig. 7a, the bilinear curve does not fit well the data in the range of f_c between 25 – 40%. To correct this situation, three methods have been developed.

One of the three methods, proposed by Chang and Deng [34], can be linked to the concept of packing potential. Chang and Deng [34, 35] believed that the predicted bilinear line is caused by the oversimplified assumption adopted in the LPDM. In LPDM, a packing of binary mixture is assumed to be built by one of the following two mechanisms: for lower content (coarse particle dominant region), fine particles are filled into the pores between coarse particles; for higher fines content (fine particle dominant region), the coarse particles are embedded into the fine particle matrix. In either case, only one type of mechanism (either filling or embedment) can occur for the binary mixture (see Eqs. 6a and 6b).

Opposite to the assumption adopted by LPDM, Chang and Deng [34] assumed that both mechanisms can occur simultaneously in a packing of mixture. Thus, the potential parameter ω is divided into two parts: the filling potential parameter ω_1 and the embedment potential parameter ω_2. Consequently, the term $\omega(e^U - e^L)$ in Eq. (5a) can be viewed as a combination of two parts: $\omega_1(1+e_2)y_2$ due to fine particles filled into the packing mixture, and $\omega_2 e_1 y_1$ due to coarse particles embedded into the packing mixture, thus

$$\omega(e^U - e^L) = \omega_1(1+e_2)y_2 + \omega_2 e_1 y_1 \tag{9a}$$

Using Eq. (9a) and Eq. (1), Eq. (5a) becomes

$$e = (e_1 y_1 + e_2 y_2) - \omega_1 (1 + e_2) y_2 - \omega_2 e_1 y_1 \quad (9b)$$

Eq. (9b) is in the same form as that proposed by Chang and Deng [35], except ω_1 and ω_2 were expressed in symbols *a* and *b*. To facilitate the notion of combined mechanism, they introduced a state parameter *x*, and both the filling potential parameter ω_1 and the embedment potential parameter ω_2 are functions of the state parameter *x*. Thus, the void ratio of mixture is a function of the state parameter *x*:

$$e(x) = (e_1 y_1 + e_2 y_2) - \omega_1(x)(1 + e_2) y_2 - \omega_2(x) e_1 y_1 \quad (10a)$$

The state parameter *x* can be regarded as the controlling size of the packing ($d_1 \geq x \geq d_2$), which governs the magnitudes of packing potential parameters ω_1 and ω_2. Chang and Deng [34] showed that these two parameters are functions of two size-ratios (between particle sizes and packing controlling size *x*), given by

$$\omega_1(x) = (1 - d_2/x)^p \quad (10b)$$

$$\omega_2(x) = (1 - x/d_1)^s \quad (10c)$$

The size ratio d_2/x governs the packing potential due to filling mechanism and the size ratio x/d_1 governs the packing potential due to embedment mechanism. The exponents *p* and *s* are two parameters corresponding to ω_1 and ω_2, respectively.

The state parameter x does not need to be known priori. According to the second law of thermodynamics, for a system reaches equilibrium at constant temperature and pressure, there is a natural tendency to achieve a minimum of the Gibbs free energy (i.e., the thermodynamic potential). Gibbs energy is proportional to the specific volume (related to void ratio by $(1 + e)/\rho_s$, ρ_s is density of solid), which is an important parameter for describing the system's thermodynamic equilibrium state. By varying *x*, the specific volume alternates. The system reaches equilibrium when the following equation is satisfied.

$$\frac{de(x)}{dx} = 0 \tag{11}$$

Thus, the solution of $e(x)$ can be solved from the set of governing Eqs. (10) and (11). This model requires only two parameters, p and s, which can be calibrated from experimental results [34].

The second method proposed by Kwan et al. [13] introduced an additional parameter (i.e. wedging effect parameter c). The wedging effect becomes significant when fine particles are enough to fill voids among coarse particles (e.g. f_c = 25 – 40%). The wedge effect is assumed to be related to the wedge parameter and proportional to the square of fines content (i.e., cf_c^2). This assumption allows the predicted relationship between e and f_c to be nonlinear so that the model is capable of modelling the nonlinear nature of data points as observed in Fig. 7a.

The interaction functions introduced by Kwan et al. [13] for the 3-parameter packing model are as follows:

$$a = 1 - (1 - r)^{3.3} - 2.6r(1 - r)^{3.6} \tag{12a}$$

$$b = 1 - (1 - r)^{1.9} - 2r(1 - r)^{6} \tag{12b}$$

$$c = 0.322 \tanh(11.9r) \tag{12c}$$

where a, b, and c refer to the loosening, wall, and wedging effects, respectively.

The third method was proposed by de Larrard [11] who considered that if a specimen is perfect compacted, a bilinear line would be achieved, and the measured curved line is due to insufficient compaction. To this end, he introduced a parameter (i.e., compaction index K). As the value of K approaches to infinity, the mixture is considered as a virtual packing being perfectly compacted. However, in real situations, the value of K usually ranges in 4.5 – 15. He proposed a method of converting from the density of a virtual packing to the density of a real packing. Thus, the real packing void ratios converted from the bilinear line through the variable K would give a curved shape. The model is called the Compressible

347 Packing Model (CPM). Recently, Roquier [33] introduced a 4th parameter (i.e., critical cavity size) within the
348 framework of CPM.

349 Among the three methods for modelling the nonlinear nature of data points proposed by Chang and Deng
350 [34], Kwan et al. [13] and de Larrard [11], both methods by Kwan et al. [13] and de Larrard [11] introduced
351 a third parameter (i.e. the compaction index or the wedging effect parameter) in addition to the loosening
352 parameter and the wall parameter. The physical meaning of the two added parameters are not related to the
353 physical meaning of packing potential. Thus, these two methods cannot be linked to the concept of packing
354 potential. It is noted that the method proposed by Chang and Deng [34] utilized the concept of packing
355 potential to model the nonlinear nature, thus it remains to be a 2-parameter model, without the need to
356 introduce a third parameter.

357 As an example, the nonlinear model by Chang and Deng [34] (i.e., Eqs. (10-11)) is now applied to model
358 the experimental results by Lade [24], $e_1 = 0.58, e_2 = 0.72$, $d_1 = 0.5\,mm, d_2 = 0.7\,mm$. The two
359 parameters p and s were determined using the method described in the reference [34] (p = 3.3, and s = 2.3).
360 The value of x computed for the data in Fig. 8a is a function of fines content as shown in Fig. 8b. The predicted
361 curve of void ratio is shown by the solid curve in Fig. 8a, which is nonlinear with respect to fines content.

362 < Fig.8 >

363 Note that the packing potential parameters ω_1 to ω_2 are independent of packing procedure as described
364 in a previous section. And these two parameters are directly related to the parameters p and s as shown in Eqs.
365 (10b) and (10c). Thus, we expect that the parameters p and s, like the packing potential parameters, are
366 independent of packing procedure.

367

5. The independence of packing procedure on the parameters *p* and *s*

To verify this hypothesis that the parameters, *p* and *s*, are independent of packing procedure, the 24 sets of sand-silt mixtures listed in Table 1 were used. The two parameters *p* and *s*, determined from experimental results under both packing procedures of achieving minimum void ratio and maximum void ratios, are compared in Fig. 9 for the 24 sets of sand-silt mixtures. For the 45-degree line, the coefficient of determination R^2 is 0.97, which indicates that the parameters are nearly independent of the packing procedure.

< Fig.9 >

Since the parameters *p* and *s* obtained for the "minimum void ratio" packing procedure are nearly the same as those obtained from the "maximum void ratio" packing procedure, only the value of *p* and *s* obtained for the "minimum void ratio" packing procedure are listed in Table 1.

The values of *p* and *s* obtained from the "minimum void ratio" packing procedure are used for the prediction of both minimum and maximum void ratios using Eqs. (10) and (11). The predicted results are plotted in Fig. 10 for the 24 sets of sand-silt mixtures. Due to the good correlation of *p* and *s* shown in Fig. 9, it is not surprised to see the good agreement between the predicted and measured results for both minimum and maximum void ratios as shown in Fig. 10.

< Fig.10 >

6. Values of parameters *p* and *s* for sand-silt mixtures

The values of *p* and *s* depend on complex factors of particle morphology such as particle shapes and surface textures. To study the range of values of *p* and *s* due to the effect of particle shapes, the 13 sets of spherical particle mixtures and the 24 sets of sand-silt mixtures listed in Table 1 are classified into 3 groups of compound particle shapes: (1) R/R, (2) A/A or SA/SA, and (3) R/A or R/SA. (R-round, A-angular, SA-

390 subangular). For the first two groups, coarse particles and fine particles have similar shapes. For the third
391 group, coarse particles and fine particles have different shapes.

392 < Fig.11 >

393 The box and whiskers plot was utilized to compare the values of p and s for the three groups of
394 compound particle shapes as shown in Fig. 11. A box and whiskers plot is composed of a box and a set of
395 whiskers. The upper whisker of the plot is the maximum of the data set and the lower whisker of the plot is
396 the minimum of the data set. The box is drawn from the first quartile to third quartile with a horizontal line
397 drawn in the box to denote the median. For the first two groups (R/R, A/A or SA/SA), the value range of p
398 and s are small compared to that of the third group (R/A, R/SA). For all three groups of compound particle
399 shapes, the range of p is greater than the range of s. The length of box also shows the same trend. The
400 median value of p is smallest for R/R, larger for A/A or SA/SA, and largest for R/A or R/SA. The median
401 value of s has the same trend.

402 From an engineering point of view, when experimental results are not available for calibration, the
403 values of p and s can be approximately estimated from Fig. 11 based on the rough descriptions of particle
404 shapes of sand and silt. To assess the accuracy for this type of estimation, we classify the values of p and s
405 into three groups. In each group, the median values are:

406 (1) R/R: p =2.8 and s =1.75 ;

407 (2) A/A or SA/SA: p =2.9 and s =2.0 ; and

408 (3) R/A or R/SA: p = 4.65 and s = 3.0.

409 The three sets of value are used for the prediction of the 24 sets of tests on sand-silt mixtures (Table 1),
410 plus the two sets of tests on glass beads and steel shots mixtures (Fig. 3). The comparisons of meausred and
411 predicted results are shown in Fig. 12a for mixtures with R/R particles shapes (glass beads and steel shots

412 mixtures), shown in Fig. 12b for sand-silt mixtures with A/A or SA/SA particles shapes, and shown in Fig. 12c
413 for sand-ssilt mixtures with R/A or R/SA particles shapes.

414 < Fig.12 >

415 The comparisons of measured and predicted results are plotted on Fig. 13a to show the degree of accuracy
416 of the predicted values compared to the measured results. Fig. 13b show the distribution of Δe (predicted e –
417 measured e). The one-standar deviation is 0.02 for mixtures with R/R particle shapes, is 0.03 for mixtures with
418 A/A or SA/SA particle shapes, and is 0.054 for mixtures with R/A or R/SA particle shapes. This can be
419 interpreted that, at least 68% of probability, the predicted error is within ± 0.02 for mixture with R/R paticle
420 shapes, within ± 0.03 for mixture with A/A or SA/SA paticle shapes, and within ± 0.054 for mixture with R/A
421 or R/SA paticle shapes. In Fig. 13b, the shaded zone is the one-standard diviation band for all 3 cases.

422 < Fig.13 >

423 **Conclusion**

424 In this paper, we aim to study the packing procedure effect on density of mixtures. We have defined a
425 packing potential index, which is a measure of volume reduction potential due to mixing of two components
426 of a binary mixtures under a packing procedure. Based on 24 sets of experiments on sand-silt mixtures
427 collected from the literature, we found that the packing potential index is significantly influenced by particle
428 size ratio (d_2/d_1) and the particle morphology of the mixture, such as particle shape, particle surface texture.
429 However, the packing potential index is nearly independent of packing procedure. Thus, packing potential
430 index can be treated as a material characterization parameter of the mixture system.

431 The packing potential for a mixture of given f_c can be mathematically linked to the particle interaction
432 parameters, which are used in the particle packing models to calculate the void ratio of a binary mixture
433 based on the upper and lower bound void ratios. Thus, we found the parameters p and s, similar to the

434 packing potential index, are also independent of packing procedure, from the analyses of 24 sets of tests
435 results on sand-silt mixtures.

436 The particle packing model approach is a two-step process: (1) develop upper and lower bounds based on
437 the given monodisperse void ratios e_1 and e_2, for packings of coarse and fine particles, and (2) determine
438 the *e* of the mixture based on the bounds, using the particle interaction function.

439 The two-step process approach has two advantages. The first advantage is to account the complex factors
440 of particle morphology (surface roughness, texture, sphericity), and the grain size distribution of silt or sand
441 by using the values of e_1 and e_2 as input data, which are obtained directly from experiments, and the
442 complex factors of particle morphology and packing procedure are manifested in these two values. Thus, the
443 model can at least capture some influence of these complex factors, which are usually not quantitatively
444 measured, and no analytical method can include these factors in a satisfactory manner.

445 The second advantage is to use the particle interaction parameters, which are largely dependent only on
446 the system of mixtures but independent of the packing procedure. This characteristic is useful for the packing
447 density model, because the same parameters and the same modelling methodology can be conveniently
448 applied to predict void ratios of mixtures under different packing procedures (e.g. the maximum and
449 minimum void ratios produced by two different processes).

450 For predicting void ratio of sand-silt mixtures, we proposed a set values for the particle interaction
451 parameters, *p* and *s*, (to be used in the nonlinear packing density model proposed by Chang and Deng [34]).
452 The values are suggested for mixtures with three types of compound particle shapes: R/R, A/A (or SA/SA),
453 and R/A (or R/SA). The comparisons between measured and predicted results show that: the error of
454 predicted values have a standard deviation of 0.02-0.03 for mixtures with compound particle shapes R/R and
455 A/A (or SA/SA), whereas, the error of predicted values have a standard deviation of 0.054 for mixtures with

456 compound particle shapes R/A (or R/SA). Thus, it is more difficult to achieve accurate predicted results for
457 the binary mixtures composed of two components with different particle shapes.

458

459 **Acknowledgement**

460 This paper was derived from research sponsored by National Science Foundation of the United States under a
461 research grant (CMMI-1917238). The support is greatly acknowledged.

462

463 **Reference**

464 [1] J.S. Reed, Principles of ceramics processing, 2nd ed., John Wiley & Sons, New York, 1995.
465 [2] L. Smith, A knowledge-based system for powder metallurgy technology, John Wiley & Sons, 2003.
466 [3] T.C. Powers, The properties of fresh concrete, John Wiley & Sons, New York, 1968.
467 [4] C.C. Furnas, Grading aggregates I: Mathematical relations for beds of broken solids of maximum
468 density, Ind. Eng. Chem. 23 (1931) 1052–1058. https://doi.org/10.1021/ie50261a017.
469 [5] A.E.R. Westman, H.R. Hugill, The packing of particles, J. Am. Ceram. Soc. 13 (1930) 767–779.
470 https://doi.org/10.1111/j.1151-2916.1930.tb16222.x.
471 [6] R.B. Aïm, P.L. Goff, Effet de paroi dans les empilements désordonnés de sphères et application à la
472 porosité de mélanges binaires, Powder Technol. 1 (1968) 281–290. https://doi.org/10.1016/0032-
473 5910(68)80006-3.
474 [7] W. Toufar, E. Klose, M. Born, Berechnung der packungsdichte von korngemischen, Aufbereitung-
475 Technik. 11 (1977) 603–608.
476 [8] A.B. Yu, R.P. Zou, N. Standish, Modifying the linear packing model for predicting the porosity of
477 nonspherical particle mixtures, Ind. Eng. Chem. Res. 35 (1996) 3730–3741.
478 https://doi.org/10.1021/ie950616a.
479 [9] P. Goltermann, V. Johansen, L. Palbøl, Packing of aggregates: an alternative tool to determine the
480 optimal aggregate mix, ACI Mater. J. 94 (1997) 435–443.
481 [10] T. Stovall, F. De Larrard, M. Buil, Linear packing density model of grain mixtures, Powder Technol.
482 48 (1986) 1–12. https://doi.org/10.1016/0032-5910(86)80058-4.
483 [11] F. De Larrard, Concrete mixture proportioning: A scientifil approach, E & FN Spon, London, 1999.

https://doi.org/10.1017/CBO9781107415324.004.
[12] J.D. Dewar, Computer modelling of concrete mixtures, E & FN Spon, London, 1999.
[13] A.K.H. Kwan, K.W. Chan, V. Wong, A 3-parameter particle packing model incorporating the wedging effect, Powder Technol. 237 (2013) 172–179. https://doi.org/10.1016/j.powtec.2013.01.043.
[14] R.K. McGeary, Mechanical Packing of Spherical Particles, J. Am. Ceram. Soc. 44 (1961) 513–522. https://doi.org/10.1111/j.1151-2916.1961.tb13716.x.
[15] M.R. Jones, L. Zheng, M.D. Newlands, Comparison of particle packing models for proportioning concrete constituents for minimum voids ratio, Mater. Struct. 35 (2002) 301–309.
[16] C.S. Chang, J.-Y. Wang, L. Ge, Modeling of minimum void ratio for sand–silt mixtures, Eng. Geol. 196 (2015) 293–304. https://doi.org/10.1016/j.enggeo.2015.07.015.
[17] C.R.I. Clayton, C.O.R. Abbireddy, R. Schiebel, A method of estimating the form of coarse particulates, Géotechnique. 59 (2009) 493–501. https://doi.org/10.1680/geot.2008.P.009.
[18] S.J. Blott, K. Pye, Particle shape: A review and new methods of characterization and classification, Sedimentology. 55 (2008) 31–63. https://doi.org/10.1111/j.1365-3091.2007.00892.x.
[19] K.A. Alshibli, M.I. Alsaleh, Characterizing Surface Roughness and Shape of Sands Using Digital Microscopy, J. Comput. Civ. Eng. 18 (2004) 36–45. https://doi.org/10.1061/(ASCE)0887-3801(2004)18:1(36).
[20] H. Wadell, Sphericity and Roundness of Rock Particles, J. Geol. 41 (1933) 310–331.
[21] C. Hettiarachchi, W.K. Mampearachchi, Effect of surface texture , size ratio and large particle volume fraction on packing density of binary spherical mixtures, Granul. Matter. 8 (2020) 1–13. https://doi.org/10.1007/s10035-019-0978-3.
[22] J. Zheng, R.D. Hryciw, Roundness and Sphericity of Soil Particles in Assemblies by Computational Geometry, J. Comput. Civ. Eng. 30 (2016) 1–13. https://doi.org/10.1061/(ASCE)CP.1943-5487.0000578.
[23] P. V. Lade, J.A. Yamamuro, Effects of nonplastic fines on static liquefaction of sands, Can. Geotech. J. 34 (1997) 918–928. https://doi.org/10.1139/t97-052.
[24] P. V. Lade, C.D. Liggio, J.A. Yamamuro, Effects of non-plastic fines on minimum and maximum void ratios of sand, Geotech. Test. J. 21 (1998) 336–347. https://doi.org/10.1520/GTJ11373J.
[25] S.L. Yang, Characterization of the properties of sand-silt mixtures, Ph.D. Thesis, Norwegian University of Science and Technology, Trondheim, Norway, 2004.
[26] A.B. Fourie, G. Papageorigou, Defining an appropriate steady state line for Merriespruit gold tailings,

Can. Geotech. J. 38 (2001) 695–706. https://doi.org/10.1139/cgj-38-4-695.

[27] Y.T. Cho, The study of GCTS triaxial apparatus function and mixing sand void ratio, Master thesis, National Taiwan University, Taiwan, 2014.

[28] S. Thevanayagam, T. Shenthan, S. Mohan, J. Liang, Undrained Fragility of Clean Sands, Silty Sands, and Sandy Silts, J. Geotech. Geoenvironmental Eng. 128 (2002) 849–859. https://doi.org/10.1061/(ASCE)1090-0241(2002)128:10(849).

[29] Y. Yilmaz, A study on the limit void ratio characteristics of medium to fine mixed graded sands, Eng. Geol. 104 (2009) 290–294. doi:10.1016/j.enggeo.2008.11.009.

[30] ASTM D4253-00, Standard test methods for maximum index density and unit weight of soils using a vibratory table, in: Annu. B. ASTM Stand., ASTM International, West Conshohocken, PA, 2006: pp. 1–15. https://doi.org/10.1520/D4253-00R06.

[31] ASTM D4254-00, Standard Test Methods for Minimum Index Density and Unit Weight of Soils and Calculation of Relative Density, in: Annu. B. ASTM Stand., ASTM International, West Conshohocken, PA, 2006: pp. 1–9. https://doi.org/10.1520/D4254-00R06E01.1.3.

[32] AASHTO, Correction for coarse particles in the soil compaction test, AASHTO Designation: T224-86, Washington, D.C., 1986.

[33] G. Roquier, The 4-parameter Compressible Packing Model (CPM) including a new theory about wall effect and loosening effect for spheres, Powder Technol. 302 (2016) 247–253. https://doi.org/10.1016/j.powtec.2016.08.031.

[34] C.S. Chang, Y. Deng, A particle packing model for sand–silt mixtures with the effect of dual-skeleton, Granul. Matter. 19 (2017) 80. https://doi.org/10.1007/s10035-017-0762-1.

[35] C.S. Chang, Y. Deng, A nonlinear packing model for multi-sized particle mixtures, Powder Technol. 336 (2018) 449–464. https://doi:10.1016/j.powtec.2018.06.008.

Caption of Figures

Fig.1. Upper and lower bounds of void ratios of a system of mixtures under a packing procedure.

543 **Fig. 2.** (a) Test results for steel shots reported by McGeary [14], (b) Test results for glass beads reported by
544 Kwan et al. [13], (c) the effect of particle size ratio on packing potential index obtained from test results on
545 steel shots and glass beads.
546 **Fig. 3.** The packing potential index for three systems of mixtures.
547 **Fig. 4.** The packing potential index versus particle size ratio for mixtures with 3 groups of compound particle
548 shapes.
549 **Fig. 5.** (a) The void ratios achieved by "minimum void ratio" packing procedure: (a-1) Silica #50-#80
550 mixture (a-2) Ottawa F95-Nevada fines mixture (a-3) Vietnam sand-silt mixture; (b) The void ratios achieved
551 by "maximum void ratio" packing procedure: (b-1) Silica #50-#80 mixture (b-2) Ottawa F95-Nevada fines
552 mixture (b-3) Vietnam sand-silt mixture.
553 **Fig. 6.** The effect of packing procedure on packing potential index for 24 systems of binary soil mixtures.
554 **Fig. 7.** (a) Definition of packing potential parameter ω for a given mixture with specific fines content, (b)
555 The packing potential parameter ω as a function of fines content.
556 **Fig. 8.** (a) The predicted void ratios for mixtures with different fines content, and (b) the calculated value of
557 state parameter x.
558 **Fig. 9.** Comparison of the parameters p and s obtained from "minimum void ratio" packing procedure and
559 from "maximum void ratio" packing procedure.
560 **Fig. 10.** Comparison of the measured and predicted maximum void ratios using the values p and s obtained
561 from the "minimum void ratio" packing procedure.
562 **Fig. 11.** Variation of parameters p and s for 24 soil mixtures listed in Table 1 and for spherical particle
563 mixtures used to produce Fig. 2.
564 **Fig. 12a.** Comparison of predicted results (with $p = 2.8$, $s = 1.75$) and measured results of mixtures with R/R
565 compound particle shapes.

Fig. 12b. Comparison of predicted results (with p = 2.9, s = 2.0) and measured results of mixtures with A/A or SA/SA compound particle shapes.

Fig. 12c. Comparison of predicted results (with p = 4.65, s = 3.0) and measured results of mixtures with R/A or R/SA compound particle shapes.

Fig. 13. (a) The comparison of the predicted and measured results, and (b) the probability distribution of the difference between predicted and measured void ratios for 3 groups of compound particle shapes.

Caption of Tables

Table 1 List of material properties for 24 sets of binary soil mixtures.

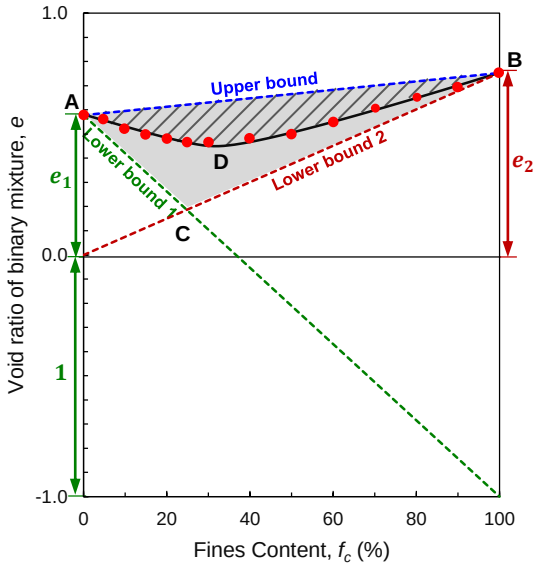

Fig.1. Upper and lower bounds of void ratios of a system of mixtures under a packing procedure.

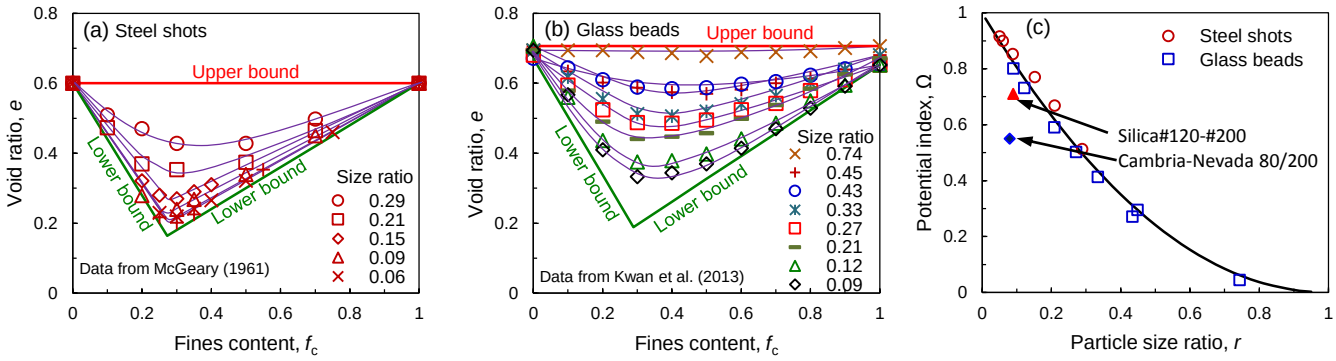

Fig. 2. (a) Test results for steel shots reported by McGeary [14], (b) Test results for glass beads reported by Kwan et al. [13], (c) the effect of particle size ratio on packing potential index obtained from test results on steel shots and glass beads.

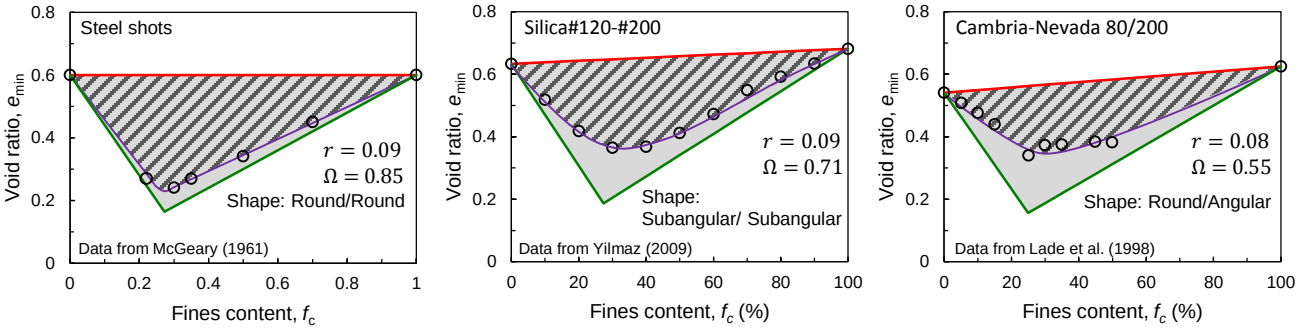

Fig. 3. The packing potential index for three systems of mixtures.

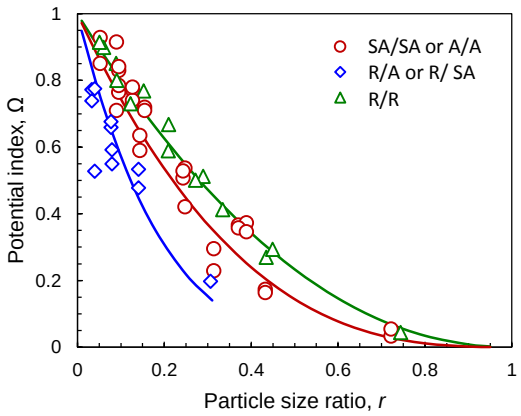

Fig. 4. The packing potential index versus particle size ratio for mixtures with 3 groups of compound particle shapes.

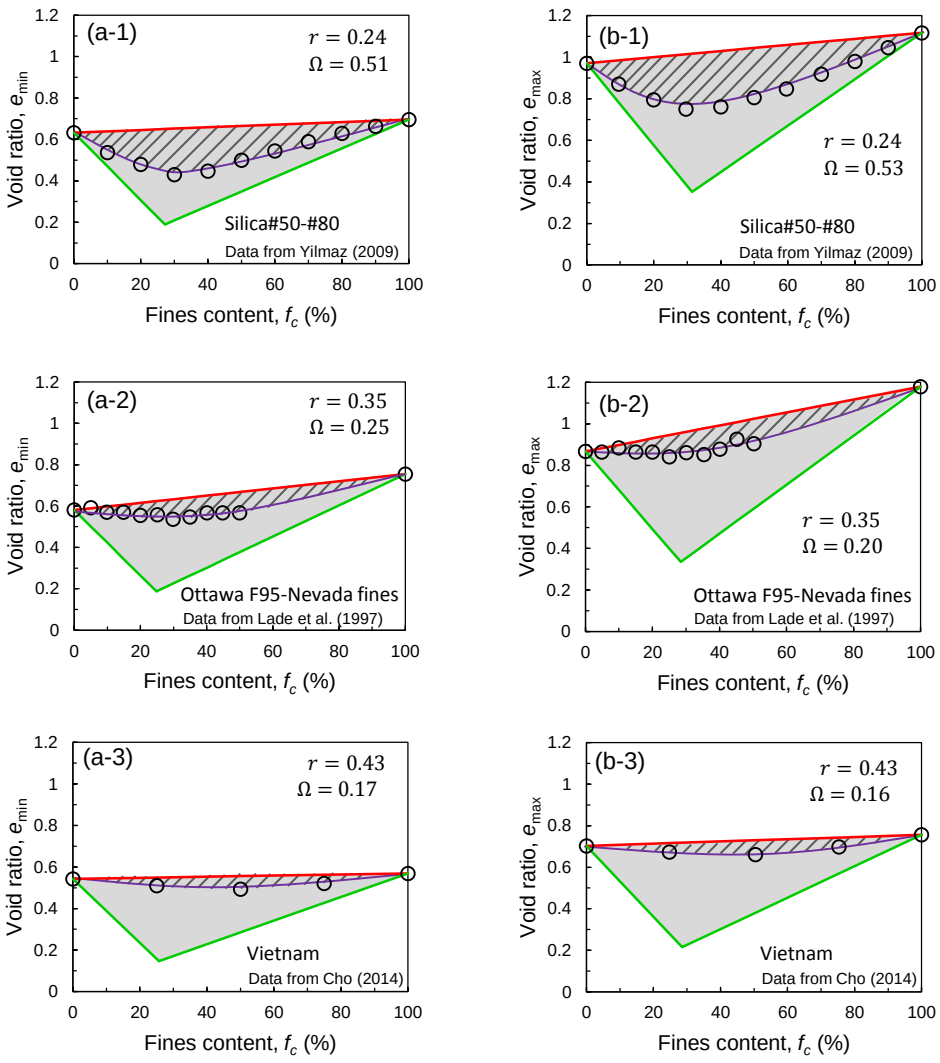

Fig. 5. (a) The void ratios achieved by "minimum void ratio" packing procedure: (a-1) Silica #50-#80 mixture (a-2) Ottawa F95-Nevada fines mixture (a-3) Vietnam sand-silt mixture; (b) The void ratios achieved by "maximum void ratio" packing procedure: (b-1) Silica #50-#80 mixture (b-2) Ottawa F95-Nevada fines mixture (b-3) Vietnam sand-silt mixture.

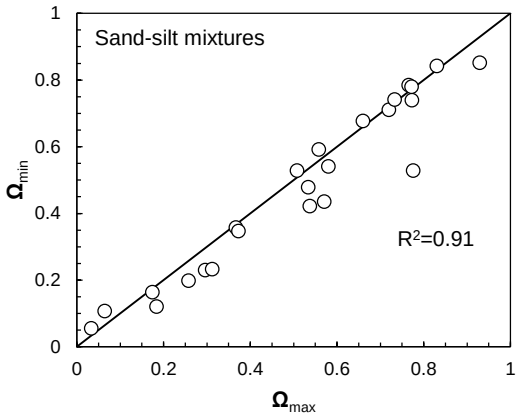

Fig. 6. The effect of packing procedure on packing potential index for 24 systems of binary soil mixtures.

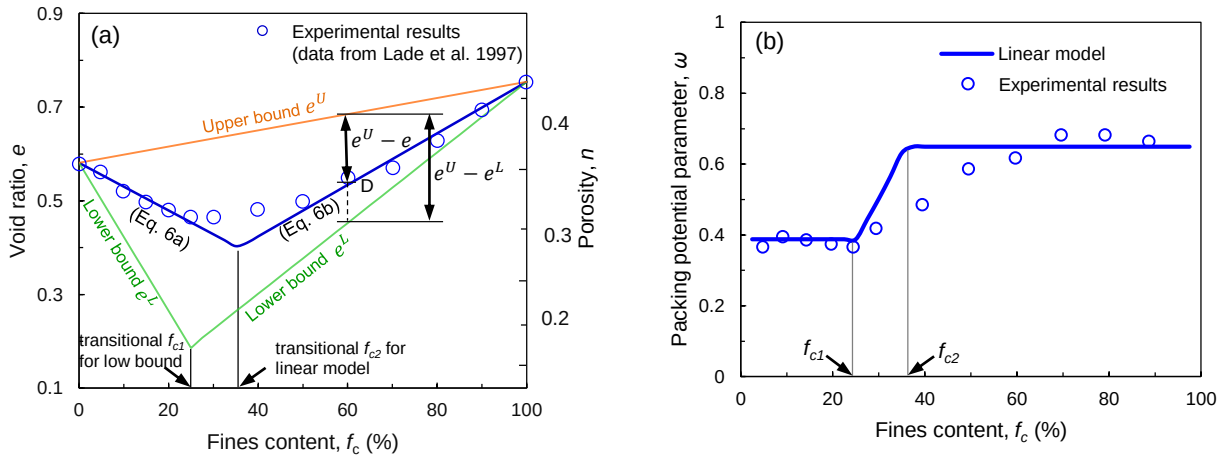

Fig. 7. (a) Definition of packing potential parameter ω for a given mixture with specific fines content, (b) The packing potential parameter ω as a function of fines content.

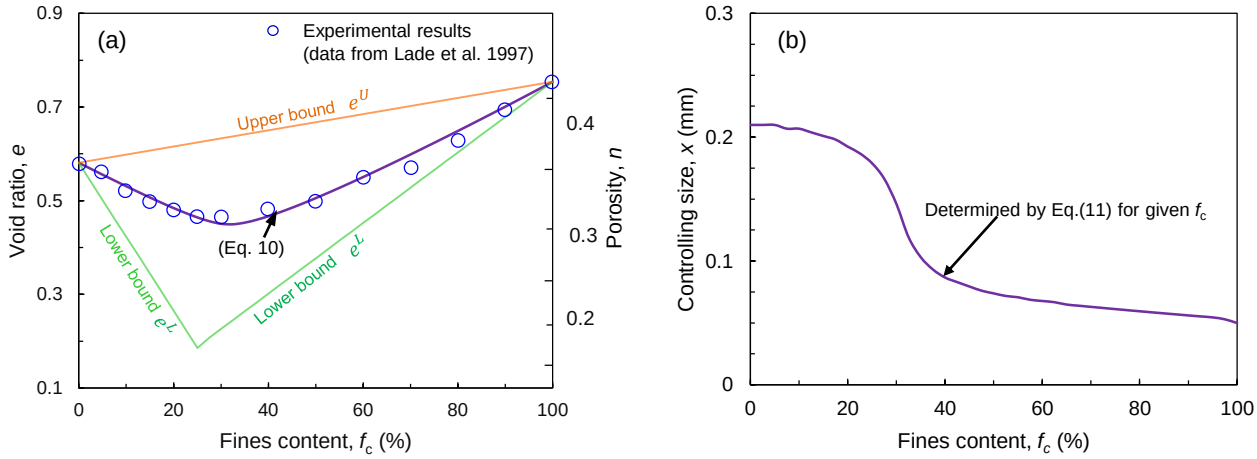

Fig. 8. (a) The predicted void ratios for mixtures with different fines content, and (b) the calculated value of state parameter x.

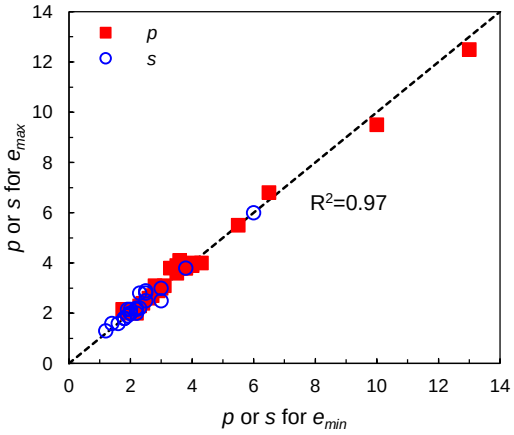

Fig. 9. Comparison of the parameters p and s obtained from "minimum void ratio" packing procedure and from "maximum void ratio" packing procedure.

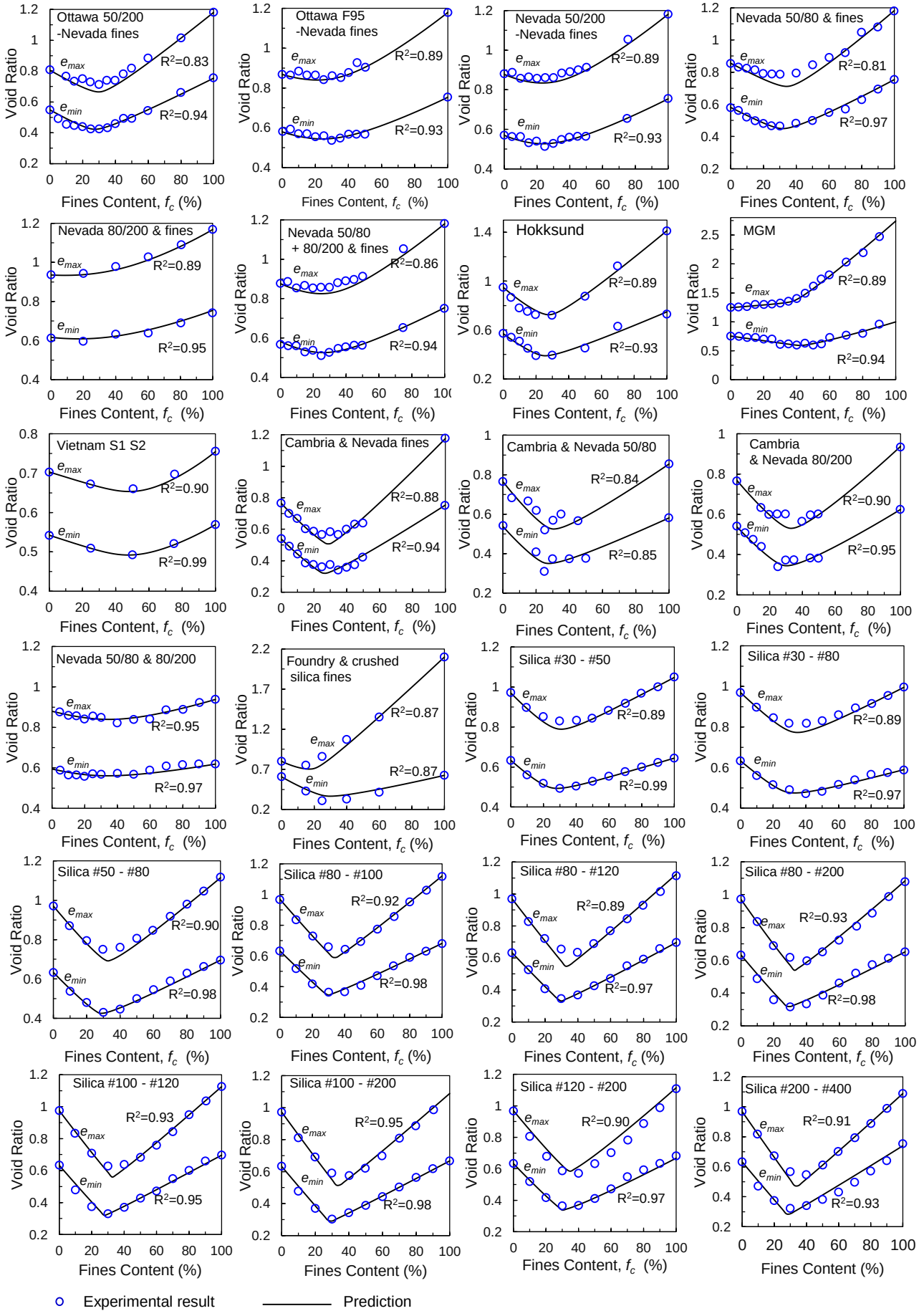

Fig. 10. Comparison of the measured and predicted maximum void ratios using the values p and s obtained from the "minimum void ratio" packing procedure.

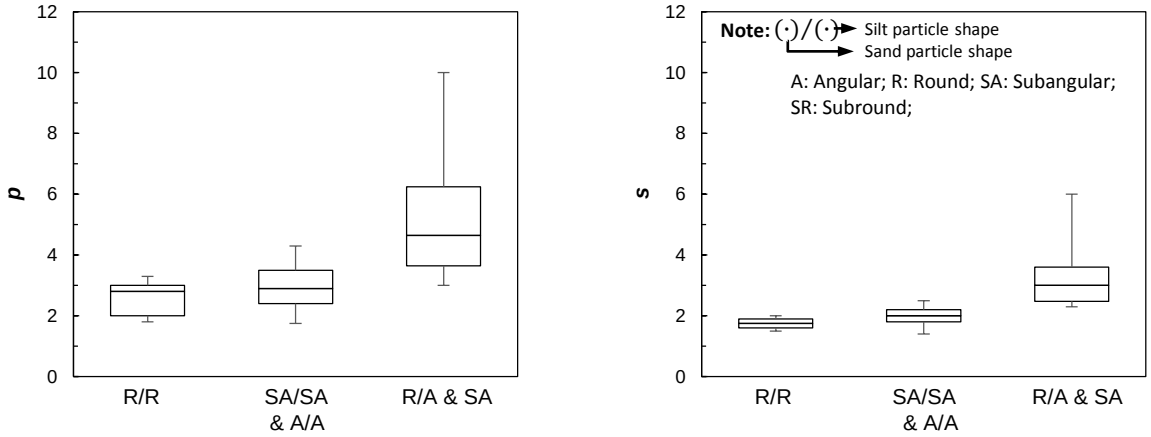

Fig. 11. Variation of parameters *p* and *s* for 24 soil mixtures listed in Table 1 and for spherical particle mixtures used to produce Fig. 2.

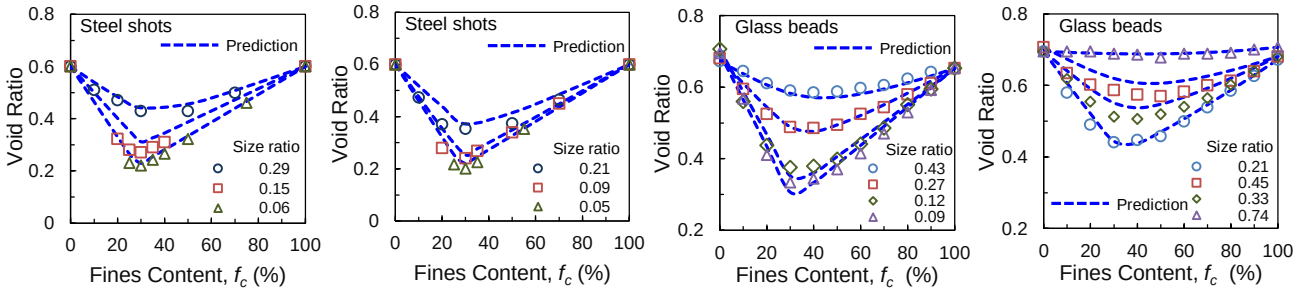

Fig. 12a. Comparison of predicted results (with p = 2.8, s = 1.75) and measured results of mixtures with R/R compound particle shapes

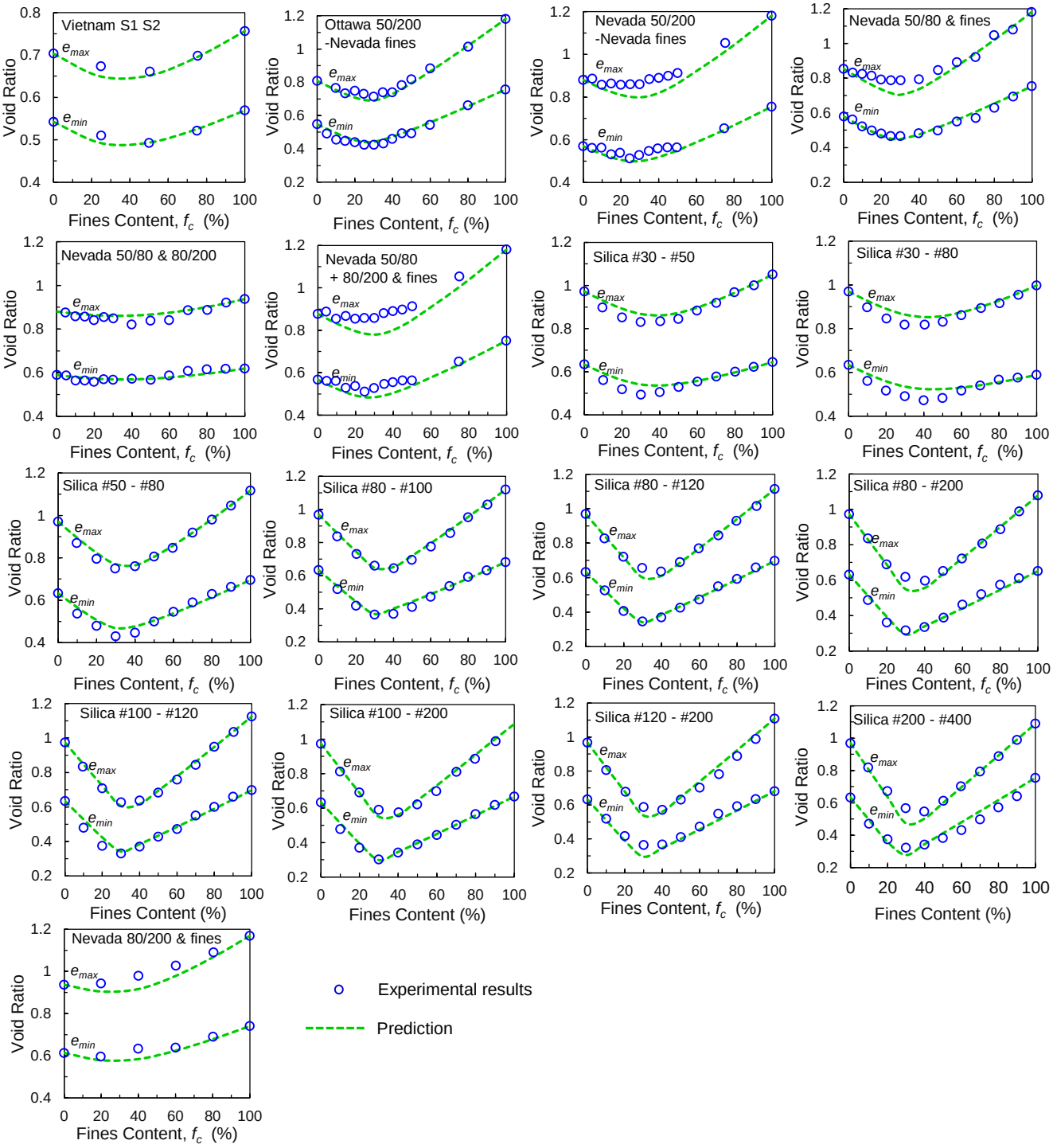

Fig. 12b. Comparison of predicted results (with p = 2.9, s = 2.0) and measured results of mixtures with A/A or SA/SA compound particle shapes.

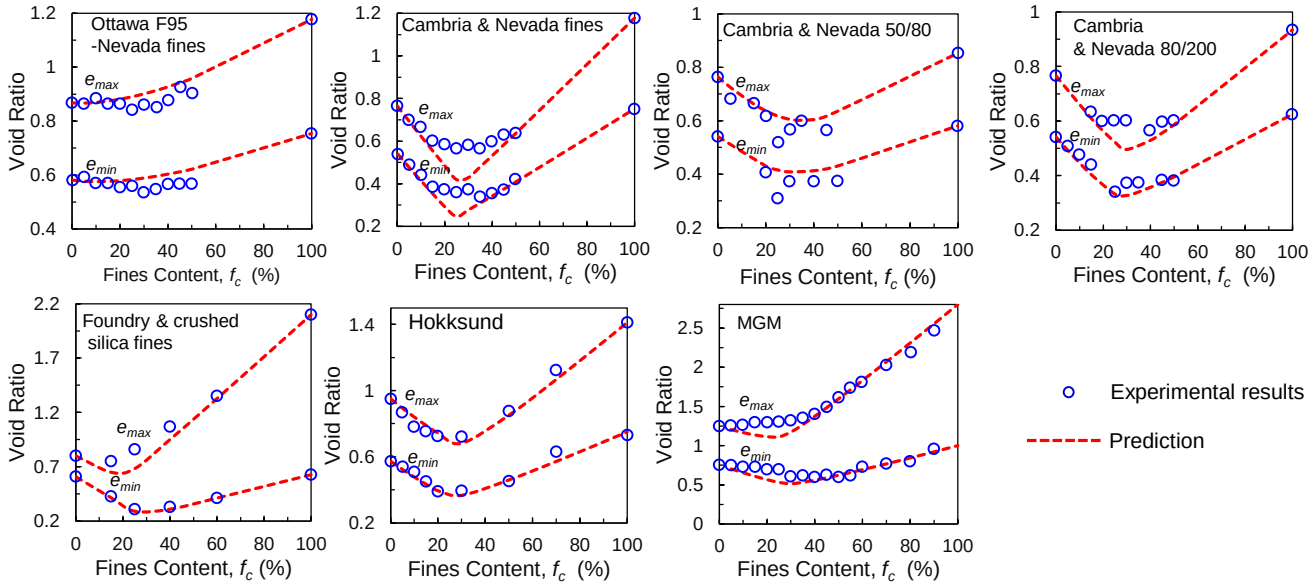

Fig. 12c. Comparison of predicted results (with p = 4.65, s = 3.0) and measured results of mixtures with R/A or R/SA compound particle shapes.

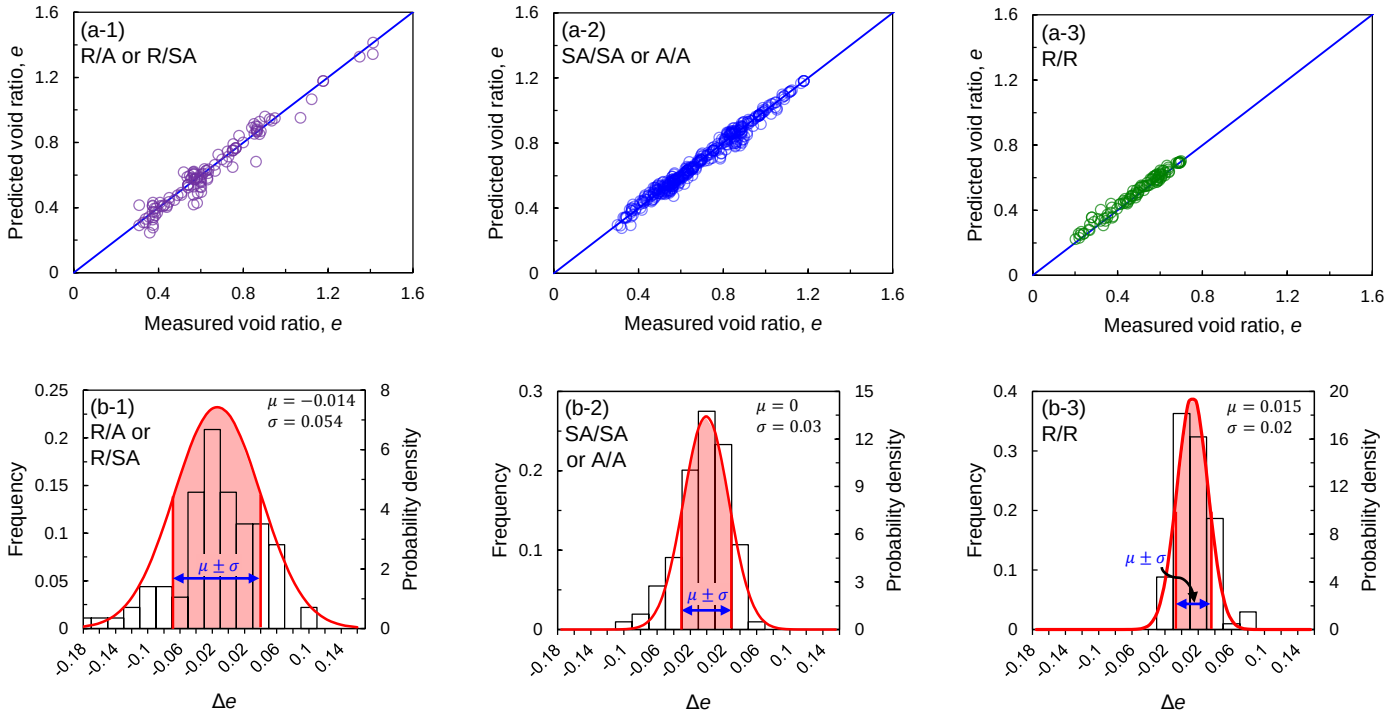

Fig. 13. (a) The comparison of the predicted and measured results, and (b) the probability distribution of the difference between predicted and measured void ratios for 3 groups of compound particle shapes.

Table 1 List of material properties for 24 sets of binary soil mixtures.

Sand/silt Mixture	Ref.	d_1(mm)	d_2(mm)	e_{min}		e_{max}		particle shape (coarse)	particle shape (fine)	p	s
				e_1	e_2	e_1	e_2				
Ottawa 50/200-Nevada fines	[23]	0.2	0.05	0.548	0.754	0. 806	1. 181	angular	angular	2.8	1.8
Ottawa F95-Nevada fines	[23]	0.16	0.05	0.58	0.754	0. 868	1. 179	subround	angular	3.6	2.3
Nevada 50/200-Nevada fines	[23]	0.14	0.04	0.57	0.754	0. 878	1. 181	subangular	angular	3.5	2.5
Nevada 50/80-Nevada fines	[24]	0.21	0.05	0.581	0.754	0. 855	1. 183	subangular to angular	subangular to angular	3.5	1.6
Nevada 80/200-Nevada fines	[24]	0.12	0.05	0.617	0.754	0. 938	1. 169	subangular to angular	subangular to angular	3.8	2.2
Nevada 50/80 - Nevada80/200+fines	[24]	0.17	0.05	0.581	0.754	0. 876	1. 180	subangular to angular	subangular to angular	3.3	2.3
Hokksund	[25]	0.45	0.04	0.57	0.76	0. 949	1. 413	sharp edges, cubical	angular, subangular	3.8	3.8
MGM	[26]	0.12	0.01	0.755	1	1. 247	2. 740	highly angular to subround	thin and plate-like	13	1.2
Vietnam	[27]	0.37	0.16	0.552	0.583	0. 703	0. 755	subangular	subangular	4	1.4
Cambria-Nevada fines	[24]	1.5	0.05	0.538	0.754	0. 765	1. 176	round	angular	10	3
Cambria-Nevada 50/80	[24]	1.5	0.21	0.538	0.581	0.765	0.854	round	subangular	3	3
Cambria-Nevada 80/200	[24]	1.5	0.12	0.538	0.624	0. 768	0. 937	round	angular	6.5	2.5
Nevada 50/80-Nevada 80/200	[24]	0.21	0.12	0.581	0.617	0. 854	0. 938	subangular to angular	subangular to angular	2.4	1.9
Foundry sand/crushed silica fines	[28]	0.25	0.01	0.608	0.627	0.8	2.1	round to subround	angular	5.5	6
Silica#16-#18 #30-#50	[29]	1.08	0.4	0.633	0.644	0. 970	1. 048	subangular	subangular	1.75	2.2
Silica#16-#18 #30-#80	[29]	1.08	0.42	0.633	0.59	0. 970	0. 996	subangular	subangular	1.9	1.9
Silica#16-#18 #50-#80	[29]	1.08	0.26	0.633	0.696	0. 970	1. 114	subangular	subangular	2.2	2
Silica#16-#18 #80-#100	[29]	1.08	0.17	0.633	0.682	0.97	1.121	subangular	subangular	2.6	1.8
Silica#16-#18 #80-#120	[29]	1.08	0.14	0.633	0.697	0.97	1.124	subangular	subangular	2.9	1.8
Silica#16-#18 #80-#200	[29]	1.08	0.1	0.633	0.651	0.97	1.084	subangular	subangular	3.1	2.5
Silica#16-#18 #100-#120	[29]	1.08	0.14	0.633	0.697	0.97	1.125	subangular	subangular	2.3	2
Silica#16-#18 #100-#200	[29]	1.08	0.1	0.633	0.668	0.97	1.084	subangular	subangular	2.7	2
Silica#16-#18 #120-#200	[29]	1.08	0.1	0.633	0.682	0.970	1.115	subangular	subangular	4.3	2.2
Silica#16-#18 #200-#400	[29]	1.08	0.06	0.633	0.7	0.97	1.091	subangular	subangular	4	2

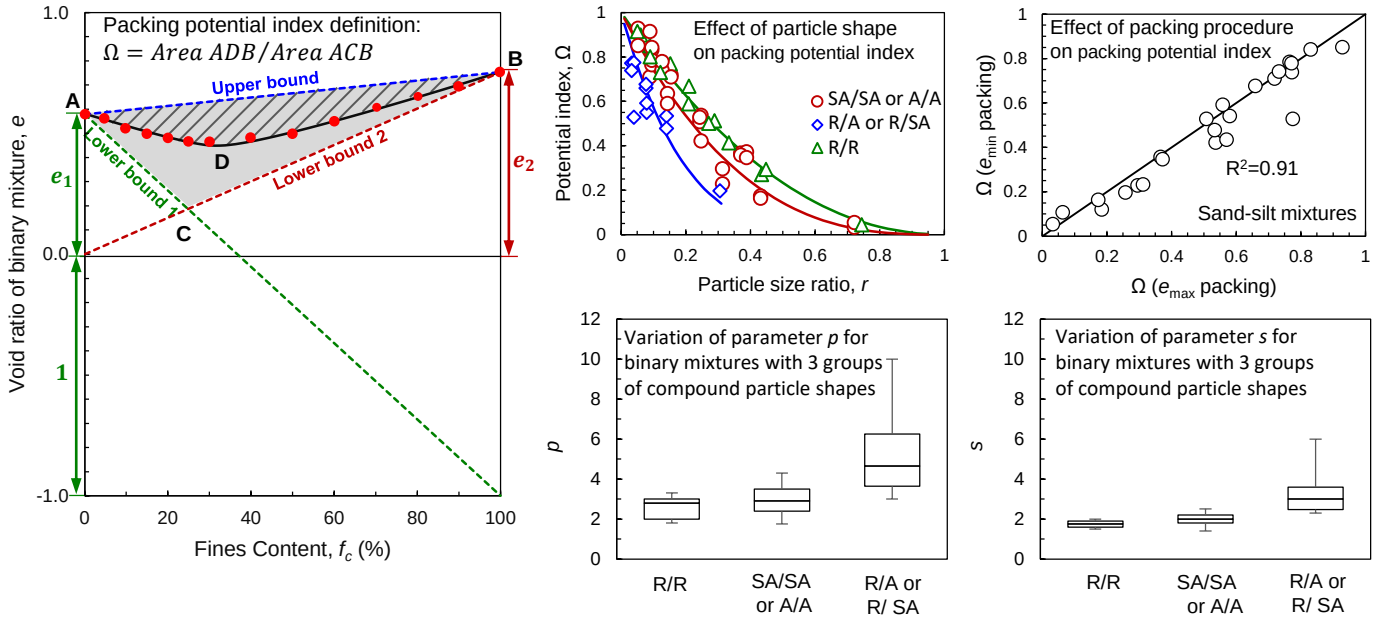

Note: $(\cdot)/(\cdot)$ → Silt particle shape; Sand particle shape A: Angular; R: Round; SA: Subangular; SR: Subround;

p and *s* are parameters related to the effect of particle morphology on packing potential